Top Curr Chem (Z) (2017) 375:69
DOI 10.1007/s41061-017-0156-1

REVIEW

Poly(aryleneethynylene)s: Properties, Applications and Synthesis Through Alkyne Metathesis

Michael Ortiz[1,2] · Chao Yu[1] · Yinghua Jin[1] · Wei Zhang[1]

Received: 17 March 2017 / Accepted: 1 June 2017 / Published online: 26 June 2017

Abstract Functional polymeric materials have seen their way into every facet of materials chemistry and engineering. In this review article, we focus on a promising class of polymers, poly(aryleneethynylene)s, by covering several of the numerous applications found thus far for these materials. Additionally, we survey the current synthetic strategies used to create these polymers, with a focus on the emerging technique of alkyne metathesis. An overview is presented of the most recent catalytic systems that support alkyne metathesis as well as the more useful alkyne metathesis reaction capable of synthesizing poly(aryleneethynylene)s.

Keywords Poly(aryleneethynylene)s · Alkyne metathesis · Conjugated polymer · Acyclic diyne metathesis · Ring-opening alkyne metathesis

1 Introduction

Acetelynic polymers have received considerable attention from polymer and materials chemists worldwide, in part due to their conductive properties stemming from an inherent electronically unsaturated and highly conjugated nature, which consequentially has led to numerous discoveries in specialty polymers with unique

This article is part of the Topical Collection "Polymer Synthesis Based on Triple-bond Building Blocks"; edited by Ben Zhong Tang, Rongrong Hu.

✉ Wei Zhang
Wei.Zhang@colorado.edu

[1] Department of Chemistry and Biochemistry, University of Colorado at Boulder, Boulder, CO 80309, USA

[2] Chemistry and Nanoscience Center, National Renewable Energy Laboratory, Golden, CO 80401, USA

functionalities [1]. One broad class of these polymers that continues to receive great attention are poly(aryleneethynylene)s (PAEs). PAEs are similar to poly(arylene-vinylene)s with a triple bond installed in place of the double bond. Alkyne linkers form much more rigid and shape-persistent linear bonds, where their alkene connections must deal with regioselectivity and rotational freedom about the double bond. It was soon realized that, due to the unique characteristics of ethynylene-based polymers, these systems hold new electronic and optical properties that would be very difficult to mimic by their olefinic counterparts [2–4].

PAEs hold structural rigidity and high thermal tolerance, while maintaining luminescent properties. Of their spectral properties, it was found that the highest occupied molecular orbital (HOMO) and lowest unoccupied molecular orbital (LUMO) energy levels, ultimately the optical band gap, of these polymers could be finely tuned by modifying the structure of the arylene moiety or by substitution of different side chains. As a result, a wide scope of applications has been studied for PAEs including photoconductivity, luminescence, chemical sensing, liquid crystallinity, biological compatibility and as porous materials.

PAEs have been generally prepared through cross-coupling reactions, e.g., Sonogashira cross-coupling. Although olefin metathesis has proven one of the most useful tools for the synthesis of vinylene-linked polymers, only recently has alkyne metathesis emerged as an attractive alternative to prepare ethynylene-linked polymers [5–9]. While olefin metathesis boasts versatile and robust catalysts, mild conditions and efficient yields (as well as a Nobel Prize), its alkyne counterpart is, comparatively, still in its infancy.

In the ensuing review, we will discuss the properties of some of the most notable functional PAE materials and their applications (regardless of the synthetic method used), and will then detail where alkyne metathesis resides in this field with a conclusive overview of current synthetic techniques used to develop these PAEs. To conclude, we will feature how alkyne metathesis has been used in combination with cross-coupling reactions to construct 2D macrocycles and how to produce cyclic oligomers as predominant single species in an effort to highlight the versatility and extensive capabilities of this emerging synthetic platform.

2 Properties and Applications of PAEs

2.1 Structure and Properties

Lower molecular weight linear PAEs (typical repeating unit is shown in Fig. 1) exhibit rigid rod-like structures in solution whereas, when the repeat unit increases these polymers, they adopt more of a flexible coil tertiary structure. Cotts and Swager examined the PAE macrostructure by light-scattering techniques and found that the rigid rod conformation begins to break down and behave as more wormlike chains at lengths of approximately 15 nm or about 20 PAE repeating units [10]. Therefore, oligomeric PAEs form rigid rods while higher molecular weight PAE polymers resemble random coils made up of these rigid subdivisions. To better understand PAE morphology in the solid-state, the main techniques used are powder

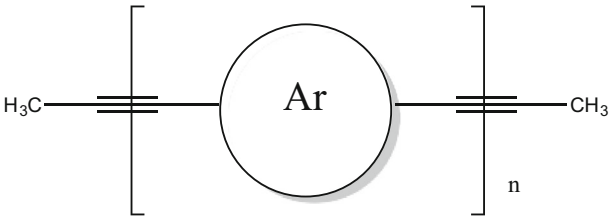

Fig. 1 Base backbone structure of linear poly(aryleneethynylene)s

diffraction and electron microscopy. From these tools, it is inferred that PAEs adopt two major structures in the bulk, interdigitated where side chains comingle between each other bringing the backbones close together, and lamellar where there is a lack of interdigitation (intermolecular interaction mainly between side chains) [11]. The trend follows: as concentration of side chains increases (increasing alkyl chain length), a more lamellar structure is assumed. Weder verified that dialkoxy-substituted PAEs can be taken up in high molecular weight polyethylene (with high solubility) and casted on to thin-films without any phase separation [12], while Langmuir–Blodgett films were successfully prepared and studied by Swager et al. who suggest that these PAEs form nanoribbons upon film fabrication [13]. The finest nanostructures have been prepared from dilute solutions evaporated slowly onto substrates. These fundamental morphological structures are of critical importance as PAEs are utilized in molecular electronics.

While Fig. 1 displays the para-substituted PAE archetype, ortho- and meta-substituted PAE systems show a variety of different characteristics including aggregation effects and response to external stimuli. One recent study conducted by Rodriguez et al. monitored the chiral nature of a series of helical PAE's functionalized at varying positions about their aryl backbones and compared induced effects from the ortho-, meta-, and para-positions [14]. On a more synthetic note, Bunz described electron-withdrawing para- and ortho-substituted moieties as activating towards palladium-catalyzed polymerization of PAEs, resulting in a higher rate of reaction and yield [15]. Conversely, ortho- and meta-substituted monomers result in generally undesirable cyclic oligomers upon polymerization through alkyne metathesis.

As mentioned above, the high degree of conjugation throughout PAE polymer systems gives rise to some of their most sought-after properties. Of these, their electronic and photophysical properties are directed by the polymer's backbone and intermolecular interactions, which dictate the delocalization of their π electrons. Overlap of p orbitals throughout the polymer allows for delocalization of the π electrons. A band of energy is then formed as atomic orbitals assimilate to form molecular orbitals. High dielectric constants in inorganic materials promote effective screening of charges and low electron binding energies, which ultimately lead to a continuous band structure of electrons that are free to redistribute and move about atoms in the presence of an external electric field. However, for conjugated polymers, electron density is not delocalized evenly across the entire chain. Therefore, these electronic properties are represented as a filled conduction

band made up of the highest occupied molecular orbitals and an empty valence band comprised of the lowest unoccupied molecular orbitals. The difference between the two is roughly consistent to the polymer's band gap (E_g) and is dependent on the repeat unit of the polymer making it a tunable property. Hence, conjugated polymers are classified as semiconducting materials.

PAEs are commonly described as wide band gap semiconductors, which absorb and fluoresce well within the visible spectrum with an absorption maximum around 350–550 nm in solution. Their optical properties vary as the dihedral angle between neighboring aryl groups increases where coplanar configurations lead to a bathochromic (red) shift in absorption and emission through increased conjugation [16–20]. In solution, the aryl units can readily rotate around the alkyne linkers due to a low barrier of about 1 kcal mol^{-1} whereas in the solid-state locked coplanarization of the aryl groups promotes further bathochromic shifts in optical spectra.

One significant property of PAEs is their characteristically high fluorescence quantum yields, as high as 0.86 in solution and 0.36 in the solid-state, which gives these polymers promise in a variety of optoelectronic applications [21]. A range of yellow to green fluorescence can be observed for typical PAEs of alkoxy or alkyl side chains. Electrical properties of PAEs are less extensively covered in the literature. It has been shown, however, that these polymers exhibit ambipolar charge transport with electron and hole mobilities on the order of 10^{-3} cm^2 V^{-1} s^{-1}, and intra-chain transport in PAE films occurs far more readily than inter-chain charge transport [21].

2.2 Applications of PAEs

2.2.1 Optoelectronics

Due to the optoelectronic properties of these PAE polymers, there is currently a great deal of research being conducted in the fields of light-emitting diodes (LEDs) and organic photovoltaics (OPVs), as well as chemical and biosensing materials.

Light-Emitting Diodes One of the most investigated fields for use of PAEs is that of LEDs, mainly due to the polymers' impressive fluorescence quantum yields as well as their high photostability. Basic LED devices are comprised of an organic semiconductor deposited on a thin-film, which is then usually arranged between an indium-doped tin oxide (ITO) anode and a metallic cathode of offset work function (Fig. 2).

LEDs utilize a phenomenon known as electroluminescence. Holes and electrons are injected into the semiconducting layer immediately following an induced external electric field. These electrons and holes can then combine in the organic material to produce a singlet excited state much like the one produced in photoluminescence, which then can radioactively decay to the ground state emitting a photon and thus the named electroluminescence phenomena. Common PAEs containing alkoxy side chains typically fluoresce in the yellow-green region of the visible light spectrum ($\lambda_{max} = 532$ nm) and require an onset voltage of about 10

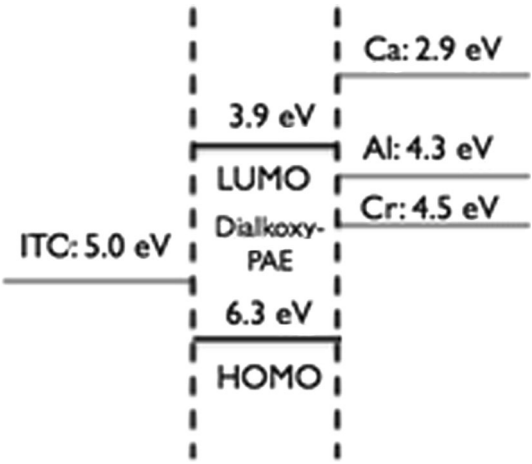

Fig. 2 Schematic representation of energy levels in a PAE-based single-layer LED device

volts while maintaining a brightness up to 80 cd m^{-2} [22]. More optimized PAE-based LEDs have recognized the low-lying HOMO of the polymer which reduces hole injection into the active layer. To overcome this, hole transport layers are introduced into the device to compensate for this energy offset [23].

These refined LED systems drastically improve device performance bringing the onset voltage down to 4.5 V while increasing the brightness output to around 250 cd m^{-2}. Despite current poly(phenylenevinylene) (PPV) and polyfluorene-based LEDs having superior device performance, PAE-based LEDs have proved much more stable than many other semiconducting materials. One additional advantage of PAE-based LEDs is the ability to tune the emission maximum by modifying the functional groups residing on the polymer backbone. Interestingly, Jin et al. reported the synthesis of a novel alternating biphenylene and fluorenediyl PAE which functioned as a uncharacteristic blue light emitter displaying an emission maximum at 473 nm [24]. Upon device fabrication, the LED exhibited a remarkable maximum brightness of 560 cd m^{-2}, far surpassing that of conventional green/yellow-emitting PAE devices.

Current strategies for improving PAE-based LEDs include the design of copolymers, particularly copolymerizing electron-rich monomers with electron-poor monomers. This approach forms a donor–acceptor type PAE material and shows much promise in the field of LEDs. Of these, Patri et al. recently prepared several polyfluorene-based PAEs copolymerized with three different electron-donating thiophene-based heteroaromatic groups [25]. These synthesized coblock-PAEs showed high molecular weight, good solubility in organic solvents and strong thermal stability along with being optically active and fluorescent while maintaining a narrow band gap. Upon LED device fabrication, these polymers exhibited an emission maximum at 600 nm with a threshold voltage of 6 V. Huang et al. managed a different approach to preparing one of these donor–acceptor-type PAE systems by functionalizing the polymer side chains with electron-withdrawing cyano-modified aryl moieties opposed to a copolymerization technique, which proved another capable LED material with narrow band gap properties [26].

In addition to working with purely ethylene-based systems, there has been some exploration into development of poly(phenyleneethynylene)-alt-poly(phenylenevinylene) (PPE-PPV) polymers first proposed by Bunz in 2000 [27]. This immediately spurred several groups to synthesize and investigate the optical properties of new PPE-PPV polymers [28–32]. These hybrid systems boast an enhanced electron affinity making electron injection easier for the electroluminescence process, thus producing low threshold materials for LED devices while holding a thermostability of up to 300 °C [33, 34].

Organic Photovoltaics Baseline requirements for typical photovoltaics and organic photovoltaics (OPVs) include efficient absorption over the visible and near-infrared spectrum (NIR), high free carrier mobilities and comparable HOMO and LUMO overlap along with bulk morphology consideration. PAEs have intrinsically high charge carrier mobilities with abilities to tune absorption in the visible and NIR region by modifying polymer backbone and side chain substituents. While there are a few examples of narrow band gap PAE polymers, the vast series of PAEs that have been developed are wide band gap, which give low to modest power conversion efficiencies upon blending with bulk heterojunction solar cells [21].

It has become clear that morphology in the solid-state greatly dictates the performance of OPV devices [35–37]. Hoppe et al. have utilized a PPE-PPV-based (electron donor) bulk heterojunction to study these effects of morphology on polymer–fullerene OPVs [38]. They found through spectroscopic, AFM and electrical characterization techniques that, while the PPE-PPV copolymer assembled into fibrillic semicrystalline phases, cell performance was very low, establishing that the presence of crystalline phases in the microstructure alone does not guarantee high efficiencies.

While most PAE involvement in OPV fabrication centers around the use of PPE-PPV copolymers, Otera et al. reported a couple of studies in the synthesis and application of anthrecene substituted PAEs as dyes in dye-sensitized solar cells [39, 40]. These polymer dyes were found to have a strong absorption band centered at 510 nm and showed good carrier mobilities (on the order of 10^4 L mol^{-1} cm^{-1}). It was found that amino- and cyano-substituted PAE side chains promoted charge separation in the excited state, thus corresponding dye-sensitized solar cells showed moderate power conversion efficiencies of 5.0%.

Chemical Sensing The highly fluorescent nature, excellent fluorescent quantum yields and high degree of tunability of PAEs make these polymers ideal candidates for sensing materials. A sensor, by definition, binds reversibly to an analyte and exhibits an observable change in a property upon complexation. Photoexcitation of the fluorescent polymer yields an excited state exciton, which can radiatively or non-radiatively relax back to the ground state. In the presence of an analyte with higher electron affinity, the excited state electron can undergo electron transfer, thus effectively quenching the photoluminescence of the polymer as utilized in fluorescence "turn-off" sensing as seen in Fig. 3. Comparatively, polymer interaction with an analyte, which enhances the photoluminescence behavior of the polymer, produces a fluorescence "turn-on" sensor.

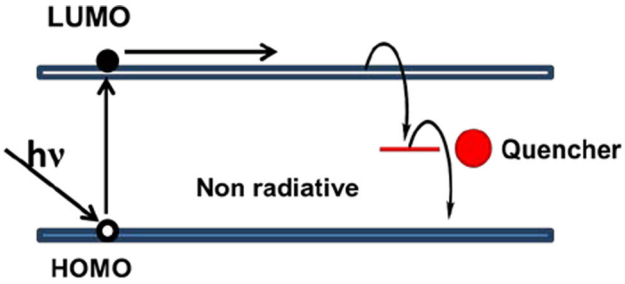

Fig. 3 Band diagram of a photoexcited conjugated polymer undergoing electron transfer to an analyte inducing fluorescence quenching [21]

Most sensing materials are developed from small molecules; however, conjugated polymers present some unique advantages to these systems. For small molecules such as organic dyes, multiple analyte interactions are necessary to produce effective quenching, and these dyes are usually only capable of binding to a single analyte, presenting issues when attempting to engineer multivalency effects [41]. Conversely, in conjugated polymers, the electron is more readily delocalized across the conjugated backbone, giving interaction with a single analyte the ability to quench the fluorescence from the whole chain. Additionally, by taking advantage of repeat units in the polymer structure, multiple points of sensory interaction are supported. Such techniques are commonly advantageous in sensing of large biologically active molecules such as proteins or bacterial cells [3].

The Stern–Volmer equation is possibly the most valuable mathematical tool in the analysis of these conjugated polymer sensing materials:

$$\frac{I_0}{I_{[Q]}} = 1 + K_{sv} \cdot [Q]$$

Here, I_0 is the fluorescence intensity of the pure polymer (without quencher Q), and $I_{[Q]}$ is the fluorescence intensity of the bound polymer and quencher at concentration [Q]. K_{sv} is the slope of the equation translating to the binding constant or also known as the Stern–Volmer constant. It should be noted that this equation holds well for static quenching, while more complicated analyses are required for instances of dynamic quenching, superquenching or ratiometric sensing. Most PAEs, however, have short excited state lifetimes and fall into the regime of static Stern–Volmer quenching.

The first significant example of fluorescence quenching of PAEs was conducted in 1995 by Swager et al. who studied the interactions between a cyclophane-appended PPE (**1**) and analyte paraquat (**2**) (Fig. 4) [42]. The binding constant K_{sv} between the PPE and analyte was found to be 1.01×10^5 M^{-1} per repeat unit base. They then constructed a cyclophane-modified monomeric small molecule dye and measured the binding constant with the same paraquat analyte, which was determined to be 1.6×10^3 M^{-1}. It was concluded that the PPE receptor, on a per active site basis, is over 60 times more sensitive than the small molecule dye. While this seminal work is not "field applicable" and is more proof of concept, the herbicide

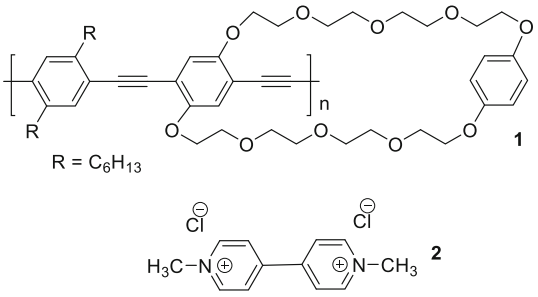

Fig. 4 The structure of Swager's cyclophane-substituted PPE and analyte paraquat

paraquat is poisonous to humans, and this study clearly established the advantages of PAEs as sensing materials, opening the doors for many new developments.

Most explosives are organic compounds containing electron-poor nitro moieties. These electron-deficient groups tend to complex well with electron-rich conjugated polymers allowing quenching of the excited state polymer by electron transfer to the low-lying LUMO of the explosive organic analyte. One of the most notable uses for PAEs in sensing technology has been the detection of explosive through fluorescence quenching, such as 2,4-dinitrotoluene (DNT) and 2,4,6-trinitrotoluene (TNT). Swager continued to improve his design, branching out from PAEs to successfully detect DNT and several other nitrated organic compounds [43–45]. More recently, Fang et al. demonstrated a new class of highly fluorescent PAEs selective towards TNT even in aqueous and salt water environments, highlighting their use in real-world applications [46]. They found that incorporating pyrene moieties into the polymer backbone (increasing electron density and thus increasing binding strength of TNT to pyrene) enhanced the polymer sensitivity by a factor of 5 compared to standard alkoxy substituted benzene rings of PPE.

Many other chemosensing applications for PAEs have been explored recently, including Thomas et al.'s impressive synthesis of novel two-dimensional PPEs (**3**–**5**) containing singlet oxygen-reactive tetracene side chains (Fig. 5) [47]. They

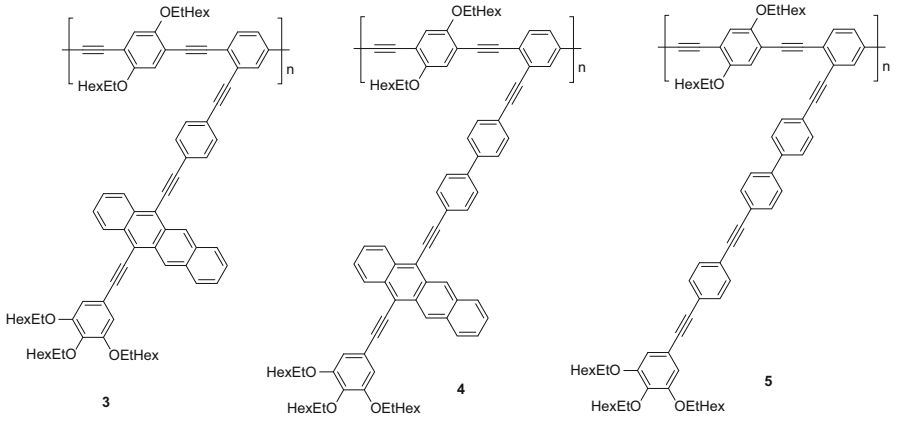

Fig. 5 Structure of the donor–acceptor-type tetracene-linked PAEs

discovered that, prior to exposure of $^1O_2$, only tetracene fluorescence at 582 nm is observed regardless of excitation wavelength. Due to the donor (polymer backbone)–acceptor (tetracene) nature of this system, energy transfer to the tetracene side chains was occurring rending solely tetracene fluorescence. However, upon oxidation of the majority of tetracene groups, a ratiometric blue-shifted 468-nm band dominated the emission spectrum as the rate of energy transfer to the oxidized tetracenes drastically decreased. By harnessing this competition between excited state relaxation processes, the researchers proposed the use of this material in the analyte-induced removal of single oxygen traps for light-harvesting materials.

2.2.2 Porous Materials

Up to this point, we have discussed a more traditional polymer motif intrinsic to PAEs of rather linear polymeric materials (granted tertiary intra- and interchain interactions). While some porous PAE-structured networks retain a two-dimensional (2D) framework, a great deal of recent attention has been shifted to three-dimensional (3D) microporous polymers [48–51]. It should be noted that these porous networks encompass a wide field including metal organic frameworks (MOFs) and covalent organic frameworks (COFs). In this review, however, we will focus on frameworks built from primarily alkyne linkers.

Gas Adsorption One of the most coveted properties of porous PAEs is their high degree of surface area inherent to the porous nature of the structured 2D and 3D networks. Porous PAE materials are commonly analyzed through Brunauer–Emett–Teller (BET) experiments to obtain sorption isotherms (usually from nitrogen gas), which give the specific surface ($m^2\ g^{-1}$, S_{BET}) of the material. The BET isotherm is related to traditional Langmuir isotherms in that the latter measures adsorption of a single layer of gas molecules where the former accounts for multiple molecular layers of a gas adsorbed to a surface. Typical surface values range from 500 to 1000 $m^2\ g^{-1}$, with more exceptional PAEs measuring around 5000 $m^2\ g^{-1}$ [48].

The first major deviation from conventional MOFs or COFs came in 2007 from the laboratory of Cooper who reported the formation of a PAE (**8**) from a mixture of triethynylbenzene (**6**) and 1,4-diiodobenzene (**7**) reactants through Pd-catalyzed cross-coupling reaction in moderate yield (65%) with BET surface areas ranging from 522 to 834 $m^2\ g^{-1}$ (Scheme 1) [52]. In this study, they recognized the ability to tailor micropore size and surface area of their PAEs by varying the length of the phenyleneethynylene struts used.

The same authors continued to explore these newly established PAE materials in an effort to increase potential surface area. They first attempted network synthesis through brominated substrates and discovered that none of these held more advantageous properties over the iodo-derived PAEs from Scheme 1 [53]. The next avenue investigated by Cooper in 2010 was the effect of solvent on the synthesis of porous PAEs [54]. Of the solvents screened (toluene, DMF, THF, and dioxane), DMF was shown to yield PAEs with BETs almost twice of those formed in toluene (1260 $m^2\ g^{-1}$) with THF only giving a slight increase of BET from toluene (940 $m^2\ g^{-1}$).

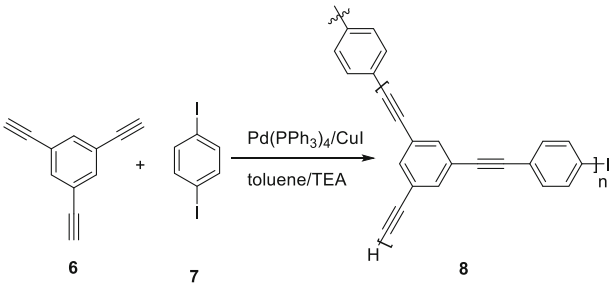

Scheme 1 Cooper's PAE synthesis through cross-coupling reaction

More recently, tetrahedral monomers have been employed to fabricate a variety of three-dimensional porous systems. In an effort to exemplify the utility of foresight through rational design at the molecular level, Zhou et al. devised a strategy to realize high surface area through careful monomer design [55]. The biphenyl monomer **9** was designed to adopt a tetrahedral conformation based on a series of side groups which geometrically lock the phenyl rings in perpendicular positions (Fig. 6). Upon polymerization and as predicted through computational simulations, the polymerized pores took on a diamond structure creating efficient surface area interaction with guest gas molecules. Impressively, one of the PAEs synthesized in this study retained a BET of 3420 m^2 g^{-1} further highlighting the importance of monomeric design in porous materials.

Catalytic Systems Due to the variety of monomers used to fabricate PAEs, a number of catalytic sites can be woven into these frameworks presenting emerging applications for PAEs as heterogeneous catalysts. The microporosity of the material allows substrates and reactants to meet with the catalytic sites and perform a series of reactions within the porous PAEs. For example, Wang and coworkers reported PAE **10** containing versatile organocatalyst, 4-(*N*,*N*-dimethylamino)-pyridine (DMAP) Fig. 7. It is reported that PAE **10** possesses highly concentrated and homogeneously distributed DMAP catalytic sites, which can efficiently catalyze acylation of alcohols with yields of 92–99%. The great advantages of using such PAEs as a catalyst are their recyclability and stability. PAE **10** can be easily recovered from the reaction mixture and reused many times (>14 consecutive cycles) without sacrificing the catalytic activity [56].

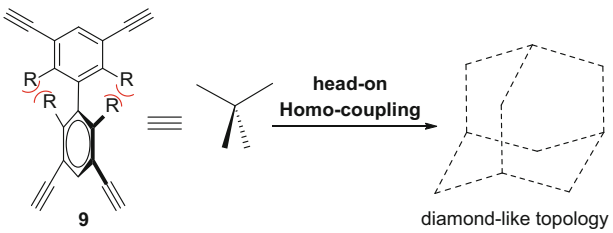

Fig. 6 Zhou's sterically-constrained tetrahedral monomer and 3D polymer of a diamond structure [55]

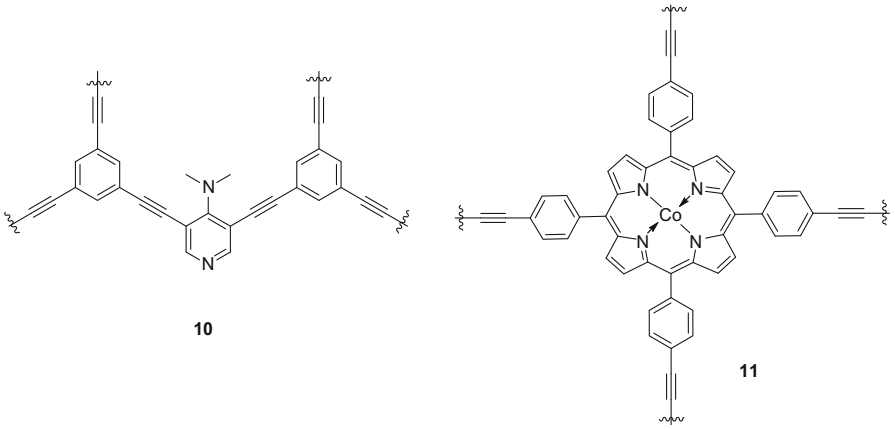

Fig. 7 Structures of catalytically active PAEs **10** and **11**

More recently, the Zhang group has applied alkyne metathesis to construct a porous Co(II) porphyrinylene-ethynylene framework **11** which was found to be highly active towards oxygen reduction reactions [57]. Upon mixing with carbon black, PAE **11** can efficiently catalyze a full reduction of O_2 to H_2O via a 4-electron pathway under both acidic and alkaline conditions, comparable to the benchmark Pt/C system. The catalyst also shows superior durability and is resistant to methanol poisoning (see Fig. 7).

Here, we conclude our survey of the many applications of PAEs. Due to these promising properties competent for functional materials, we continue this review by investigating the current synthetic methods used to produce PAEs, namely, alkyne metathesis.

3 Synthetic Methods

3.1 Cross-Coupling Reactions Versus Alkyne Metathesis

Up to this point, we have discussed the wide range of functional materials that can be fabricated from PAEs. The majority of these studies utilize the robust and well-defined palladium-catalyzed Sonogashira coupling reaction to cross-couple terminal alkynes and aryl halide monomers (commonly aryl iodides) to give ethylene-linked PAE polymers. This ubiquitously used synthetic technique was first established by Sonogashira and Hagihara in 1975, and offers a vast substrate scope, mild reaction conditions, low catalyst loadings, and produces high molecular weight polymers [58]. While the Sonogashira reaction is the choice procedure for most PAE syntheses, the method carries some inherent problems that can affect polymer performance. One of the most common issues is the retention of Pd metal in the polymer through coordination to multiple alkyne units, which results in network formation between independent polymer chains. Since such network formation

ultimately reduces overall solubility of PAE products, it can be problematic when solution-processible linear PAE is desired. Additionally, a number of defect states can be produced including dehalogenation resulting in short PAE chains and diyne defects as well as phosphoruium salt formation at the polymer's terminal positions. Due to the mechanism of polymer formation through Sonogashira coupling, this reaction is fundamentally irreversible, and so any undesired defects that arise during polymerization are generally difficult to remove from the final product.

The above-mentioned drawbacks of palladium catalyzed couplings have turned some attention toward alkyne metathesis as an efficient route for acetelyne-based polymerization [59]. The Zhang group has recently put forward an interesting comparison study on PAE porous networks synthesized between the irreversible traditional Sonogashira coupling technique and reversible alkyne metathesis [60]. The authors demonstrated the synthesis of PAEs **13** and **17** through the two competing methods as shown in Scheme 2. Each was fully characterized by FT-IR, solid-state ^{13}C NMR, TGA, SEM, and X-ray diffraction. Nitrogen adsorption measurements were also taken on the corresponding polymers and BET-specific areas were obtained and compared. As expected, 3D networks yielded higher specific surface areas compared to 2D networks for both sets of polymers. Upon comparison of polymers generated by reversible alkyne metathesis (RAM) and irreversible cross-coupling (ICC), however, a stark distinction became clear. Thermal stability of the RAM networks, **13-RAM** and **17-RAM** proved to be considerably higher than that of ICC networks, **13-ICC** and **17-ICC** (T_{dec} >600 °C vs. T_{dec} = 400 °C) and BET surface areas of RAM networks were determined to be

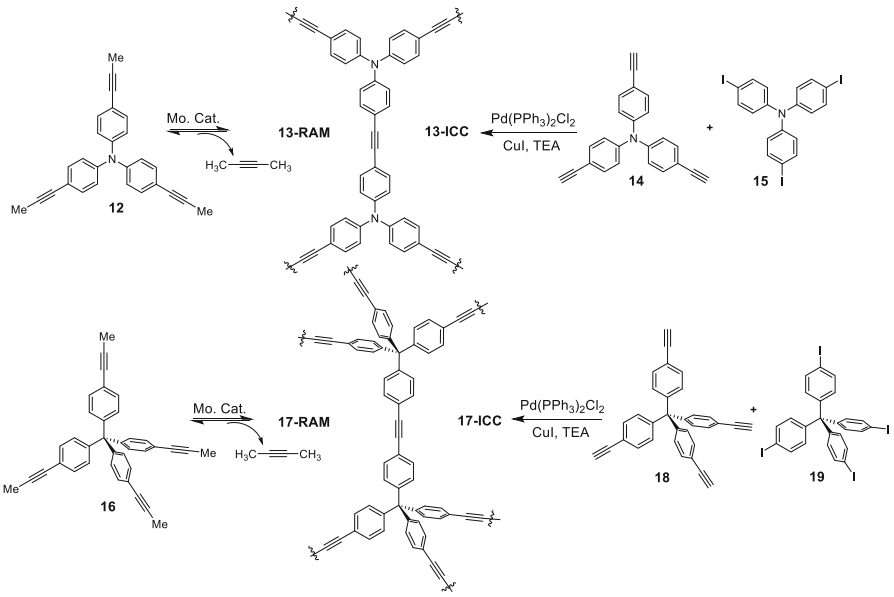

Scheme 2 Two-dimensional and three-dimensional conjugated microporous networks synthesized through irreversible cross-coupling reaction and reversible alkyne metathesis reaction

over twofold higher than those of ICC-synthesized polymers with the top performing polymer showing specific surface areas of 2312 m^2 g^{-1}. It was inferred through the article that the reversible nature of the alkyne metathesis technique allowed for self-correction of defects in the PAE networks, thus affording a more uniform porous material. Such PAEs were found to be able to adsorb a significant amount of common aromatic solvents, e.g., up to 723 wt% of nitrobenzene, suggesting their potential to absorb oil from water [61].

While this is just one example of alkyne metathesis applied to the synthesis of functional materials out of the wide variety of PAE applications, it provides a sound reason to continue the investigation of using alkyne metathesis to construct new PAE systems. Given the inherent reversibility of the metathesis reaction, alkyne metathesis offers an interesting alternative that could address those issues faced by Sonogashira polymerization.

3.2 Alkyne Metathesis Catalysts

In the past two decades, great strides have been made to alkyne metathesis field, from catalyst design to substrate scope [5, 6, 62, 63]. While the main hindrance to ubiquitous use of this metathesis technique is the availability, robustness and efficiency of the catalysts, a brief chronicle of the main catalysts leading up to the current generation should facilitate a firm introductory understanding of this field.

It was in 1968 that Pennella et al. first utilized a WO_3 catalyst on silica to transform 2-pentyne into a mixture of 2-butyne and 3-hexyne [64]. This was, however, uncelebrated due to the harsh reaction conditions (200–450 °C). Several years later, in 1974, it was Mortreux and Blanchard who demonstrated semi-efficient scrambling through the use of a homogeneous catalytic mixture of [$Mo(CO)_6$] and resorcinol (**20**, Fig. 8) when heated at 160 °C. [65] While much research has been published on derivatives of this system, the undeniable drawback of the catalyst remains its low functional group tolerance [66–77].

It was 8 years later when Schrock published a new class of tungsten alkylidyne complexes, namely a [$Me_3C{\equiv}CW(OCMe_3)_3$] (**21**, Fig. 8) system synthesized from widely available WCl_6 [78–80]. However, the Schrock-type catalyst still suffered from relatively low reactivity and high reaction temperatures, high catalyst loading, and limited substrate scope.

Following a great deal of speculation about the exact mechanism of metathesis, it was Katz (Scheme 3) who first proposed the formation of an alkylidyne complex which metathesizes acetylenes through a metallacyclobutadiene intermediate [81].

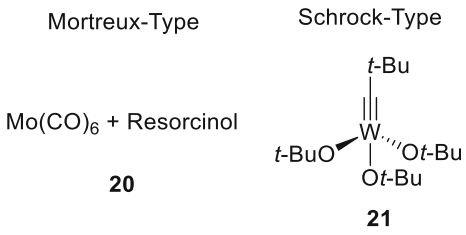

Fig. 8 Classic Mo- and W-based alkyne metathesis catalysts

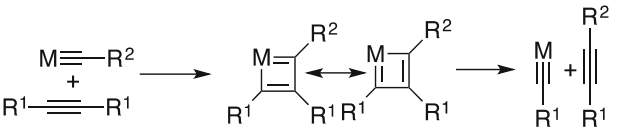

Scheme 3 Alkylidyne mechanism of alkyne metathesis

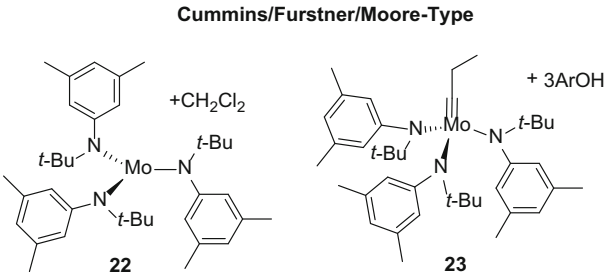

Fig. 9 Cummins, Fürstner and Moore's general type Mo-based alkyne metathesis catalysts

Beginning in the 1990s with continued evolution through the turn of the century, a new generation of molybdenum-based alkyne metathesis catalysts emerged first from the efforts of Cummins and Fürstner who developed the synthesis and analysis of the general type Mo[N(*t*-Bu)Ar]$_3$ (**22**) system, which can be metathesis-active upon treatment with CH_2Cl_2 (Fig. 9) [82–85]. Further refinement of the molybdenum precursor preparation was achieved soon after by the Moore group, developing a reductive recycle synthetic strategy to form metathesis inactive precursor [EtC≡Mo{N(*t*-Bu)Ar}$_3$] (**23**) [86, 87], which they later used to design a more advanced and active catalytic system through in situ alcoholysis with 3 equiv. phenols or alcohols [88]. Most of these trialkoxymolybdenum(VI) alkylidyne catalyst species showed efficient alkyne metathesis activity at lower temperatures and catalyst loadings with enhanced functional group compatibility.

More recently, the Zhang group has developed a highly active catalyst system comprised of a molybdenum(VI) trisamide precursor (**23**) and triphenol ligand (**25**–**27**) which, upon complexation in situ, renders the active alkyne metathesis catalyst (Fig. 10). This catalyst with multidentate ligand not only exhibits high turnover efficiency, low reaction temperatures (40–70 °C) and is compatible with a wide variety of functional groups but also has been shown to inhibit polymerization of small molecule metathesis byproducts (commonly 2-butyne). Such active catalysts showed impressive yields for a variety of transformations, including homodimerization, ring-closing metathesis, and cyclooligomerization reactions.

Perhaps more useful, this particular system showed exceptional stability upon formation, and the authors state that it remains active in solution for months at room temperature. It should be noted that this catalyst architecture was purposely designed to prevent underside coordination of small alkynes to the active molybedenum center. This feature selectively inhibits the polymerization of small molecule metathesis byproducts (2-butyne), and such a design can be seen in several

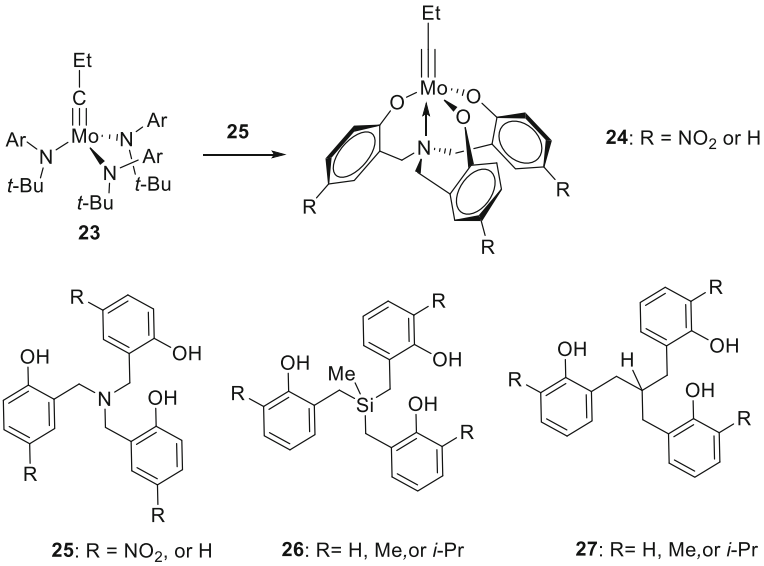

Fig. 10 Multidentate ligands and molybdenum(VI) alkylidyne catalysts

of our alkyne metathesis catalyst systems leading to the methine-based ligand (**27**; Fig. 10) exhibited in this most recent work. [89–93].

Further illustrating the versatility of these multidentate Mo(VI) carbyne catalytic systems, namely **23** and **26**, a recent study employs the active coordinated silane-ligand, molybedenum-based catalyst to prepare solution processable functional polydiacetylenes (PDAs) [94]. Such a mechanism of polymerization followed acyclic enediyne metathesis (AEDMET), which resulted in polymers with tunable physical and electrical properties through rational side-group selection. Bulk heterojunction organic solar cells were fabricated from these soluble polymers as proof of concept, highlighting the dynamic scope of metathesis-active monomers available through these catalysts.

On other systems, a pincer ligand-based tungsten alkyne metathesis catalyst (**28**) has recently been reported by Veige et al. in a study where they demonstrate the new catalyst's propensity toward forming macrocyclic polyenes in high yields [95, 96]. They claim that the catalyst functions by tethering the ends of the polymer to the tungsten center to overcome the inherent entropic price of cyclization. The proposed ring-expansion polymerization mechanistic scheme of metathesis is displayed in Scheme 4.

Unfortunately, the development of new alkyne metathesis catalyst remain scarce to this day and, in the past 5 years, only limited advancements have been made in this field. More notable catalyst systems that we discuss below in more detail are the molybdenum carbyne complexes (**29**) displayed in Scheme 5 originating from the Fischer group last year (see "ROAMP" section). For more comprehensive reviews concerning the design of alkyne metathesis catalysts, we

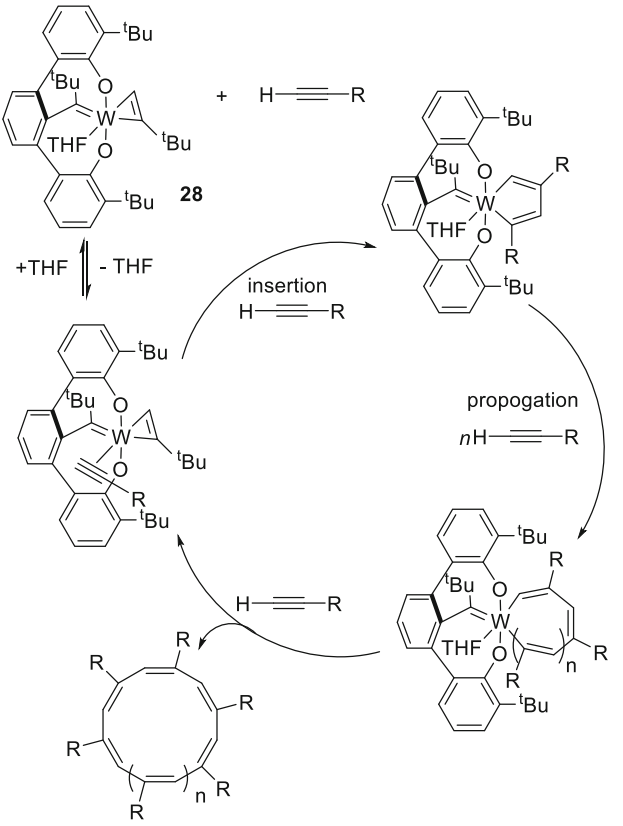

Scheme 4 Ring-expansion polymerization with tungsten-based catalyst **28** and formation of macrocyclic polyenes

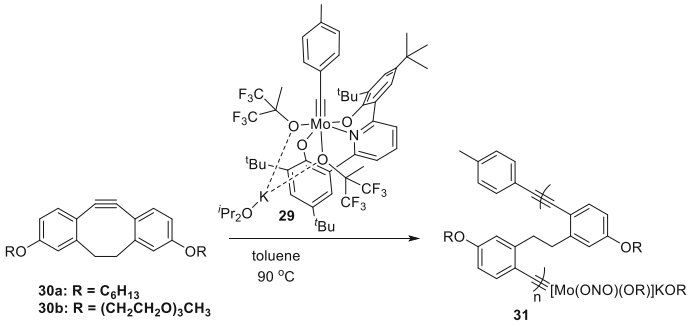

Scheme 5 Synthesis of polymer **31** using the catalyst **29**

would refer the reader to a few publications reported in the past few years [5, 8, 9].

3.3 Recent Alkyne Metathesis Techniques

3.3.1 Acyclic diyne metathesis polymerization (ADIMET)

Given the advantages of alkyne metathesis over cross coupling reactions, ADIMET has been used for the preparation of PAEs for two decades. Early work of pioneers such as Bunz and Müllen has been summarized by previous publications [5, 11, 59], and thus are not included in this review. In 2013, Zhang and coworkers have expanded the utilization of ADIMET from one-dimensional (1D) polymers to 2D and 3D polymer networks (**11** in Fig. 7, and **RAM-13**, **17** in Scheme 2) [60].

3.3.2 Ring-opening alkyne metathesis polymerization (ROAMP)

Ring-opening alkyne metathesis polymerization (ROAMP) has also attracted increasing attention as the library of available highly active alkyne metathesis catalysts expanded. The first reported ROAMP was conducted by Schrock and coworkers in 1987 [97, 98]. However, the high molecular weight polymers they produced suffered from high polydispersity (PDI >4), suggesting the need of a catalyst that could distinguish between the strained alkyne bonds in cyclic monomers and those internal alkyne bonds in polymers. Nuckolls and coworkers have reported systematic studies on ROAMP and developed an effective ROAMP system that can tolerate water, alcohols and phenolic substrates. This part of work has been covered in our previous review article [59] and thus will not be discussed in detail. [99–102].

In the past 3 years, since the publication of our last review [59], Fischer and coworkers have been the main contributors to this field. As shown in Scheme 5, Fischer and coworkers found that a pseudo-octahedral molybdenum benzylidyne ONO pincer complex $[TolC{\equiv}Mo(ONO)(OR)]{\cdot}KO^{i}Pr_2$ ($R = CCH_3(CF_3)_2$) **29** is able to catalyze ROAMP [103]. The permanently bound electron-donating tridentate ligand irreversibly blocks one of the catalyst's active sites, which prevents undesired alkyne polymerization reactions, and further increases the stability of the catalyst against air and moisture. Additionally, the reversible coordination of KOR prevents undesired chain termination and transfer processes. Both features largely facilitated the practical usage of the catalyst, as shown in Scheme 5, which produces high molecular weight polymers with exceptionally low PDIs (1.02). In addition, the authors prepared amphiphilic block copolymers (PDIs <1.07) using such a catalyst.

Very recently, Fischer and coworkers discovered that the difference of steric bulkiness of the end group of the ROAMP catalyst is accounted for the topology of the final conjugated polymer [104]. As shown in Scheme 6, starting from a highly strained cyclic alkyne **32**, two types of fully conjugated polymers can be produced based on the selection of catalysts used for the ROAMP reaction. It was found that the Mo catalyst (**34a**) with a mesityl end group yields a linear polymer **33a**

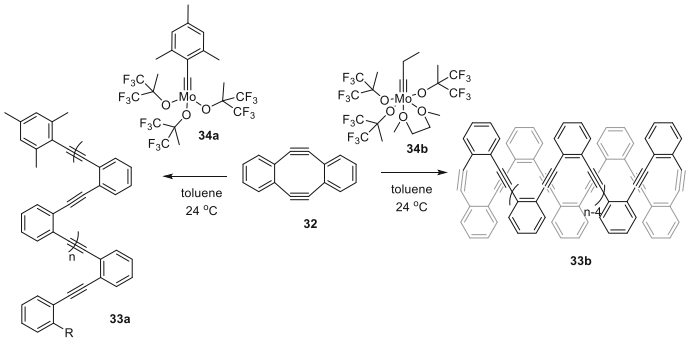

Scheme 6 Synthesis of linear polymer **33a** and cyclic polymer **33b** using alkyne metathesis

(PDI <1.7), whereas **34b** with an ethyl end group yields cyclic polymers **33b** ranging in size from $n = 5$ to $n = 20$ monomer units.

3.3.3 Combination of Cross-Coupling Reaction with Alkyne Metathesis

As previously stated, alkyne metathesis is a reversible and equilibrium controlled process. Therefore, at equilibrium, the most thermodynamically favored species dominate to reach energy minima of the system. This unique character is pathway-independent and thus provides an interesting opportunity to convert the products of irreversible reactions to more thermodynamically stable species when the reversibility is offered. In such way, we can take advantages of both kinetically controlled process and thermodynamically controlled process.

Moore and co-workers reported the first example of such a unique combination of conventional kinetically controlled cross coupling with thermodynamic controlled alkyne metathesis. They firstly prepared homo-polymer **37a/b** (**37a**, Mn = 8.5 kDa, PDI = 1.7; **37b**, Mn = 6.4 kDa, PDI = 1.8) through cross-coupling reaction (Scheme 7) of dihalide (**35**) and diacetylene (**36**). The homo-polymers were used as starting materials for the alkyne metathesis reaction without further purification. Alkyne-metathesis-mediated depolymerization of **37a/b** provided tetrameric macrocycles **38a/38b** in good yields [105, 106]. One of the great advantages of this approach compared to the direct metathesis of alkyne monomers (e.g. **39**) is that, with this cross-metathesis method, there is no need for scavenging additives or extra steps in the reaction to ensure byproduct removal. For example, in most alkyne metathesis, the metathesis byproduct, 2-butyne or PPT–≡–PPT, has to be removed to drive the equilibrium toward product formation. Although these alkyne byproducts can be removed by applying vacuum (for volatile alkynes, e.g., 2-butyne) or precipitation (for low solubility butynes, e.g., PPT–≡–PPT), these methods limit the reaction scalability and are also not atom-economic, especially in the case of precipitating large byproduct PPT–≡–PPT.

Another advantage of the above approach is the possibility of introducing multiple repeating monomer units into macrocycle backbones. For example, macrocycle **42** with two different repeating units, carbazole and phenylene, can be

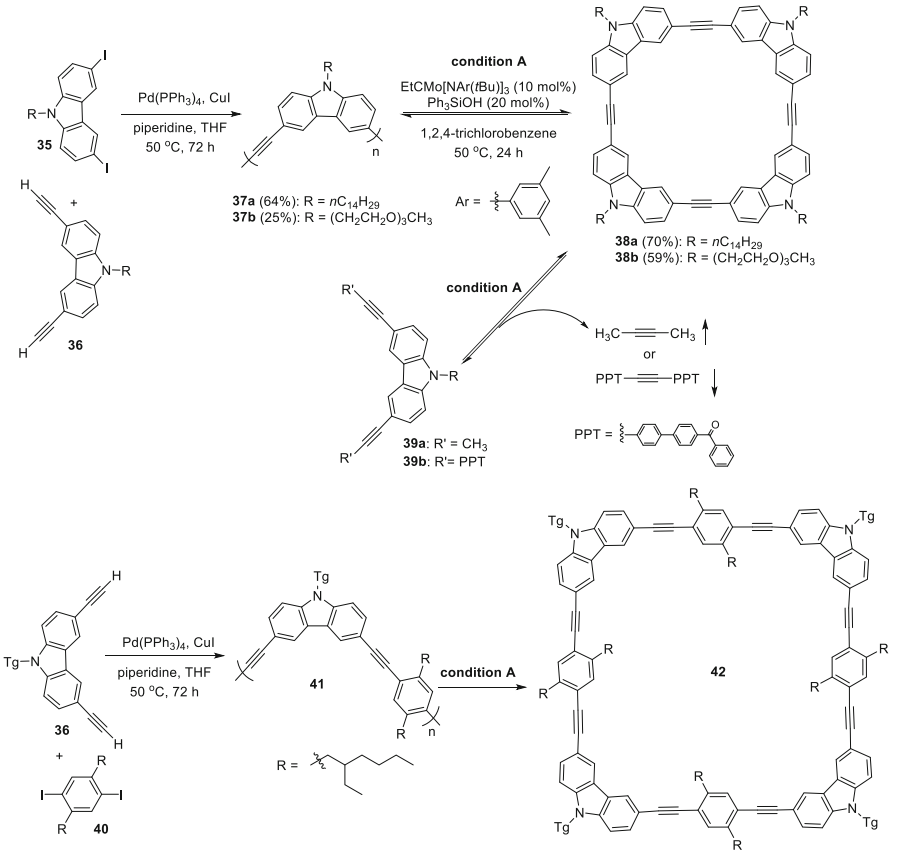

Scheme 7 Alkyne metathesis depolymerization of the polymers obtained through cross-coupling reaction to form macrocycles

obtained from copolymer **41**, which was prepared through cross-coupling of diacetylene **36** and diiodide **40**. Such a hybrid macrocycle might be hard to prepare directly from two corresponding alkyne monomers, due to the increased statistics of forming undesired oligomers and polymers with a random connection sequence of two monomers. The depolymerization strategy of polymers formed through cross-coupling reactions to macrocycles represent an interesting example of combining irreversible cross-coupling with reversible covalent reactions.

3.3.4 Cyclooligomerization

It was Grubbs who first demonstrated such depolymerization to yield cyclic oligomers through olefin metathesis [107]. The seminal study brought to light several key points including the dynamic nature of the metathesis reaction as well as the ability of metathesis to self-correct once previously established bonds in favor of a more thermodynamically stable overall structure. Moore et al.

continued this study as it applies to alkyne metathesis, with simple 2D alkyne-linked macrocycles which were synthesized from an acetylenic polymer previously prepared through Sonogashira coupling (Scheme 7) [106]. The driving force for these cyclic oligomer formations has been shown to be thermodynamic stability of the final macrocycles and metathesis' propensity towards the thermodynamic product at equilibrium [108]. This depolymerization through alkyne metathesis also supports the formation of 3D cages, which have shown interesting host–guest chemistry and electron-transfer dynamics [109–113]. While a nice library of such unique structures is growing [114, 115], to conclude, we will highlight a single study.

The novel interlocked aryleneethynylene-based cage system **44** (Scheme 8) was synthesized by our group as the first example of a thermodynamically controlled synthesis of an interlocked organic cage retaining high stability [116]. At the initial stage of the reaction, various cyclic or linear oligomeric and polymeric intermediates form. However, similar to the depolymerization approach, these intermediates gradually convert to the interlocked species. Such a complex possesses surprising thermodynamic stability over other cyclic or linear polymers or even the isolated individual cage in solution leading to its formation upon reaching equilibrium through this dynamic alkyne metathesis reaction. When a closed structure is targeted (e.g., macrocycles, or molecular cages), it is critical to design angular monomers (e.g., **39** or **43**) that can amplify the energy difference between undesired intermediates and targeted product. The presence of enough energy gap between various possible products ensures the predominant formation of the most stable species through error-correction mechanism enabled by reaction reversibility. We present this 3D aryleneethynylene synthesis to further emphasize the versatility

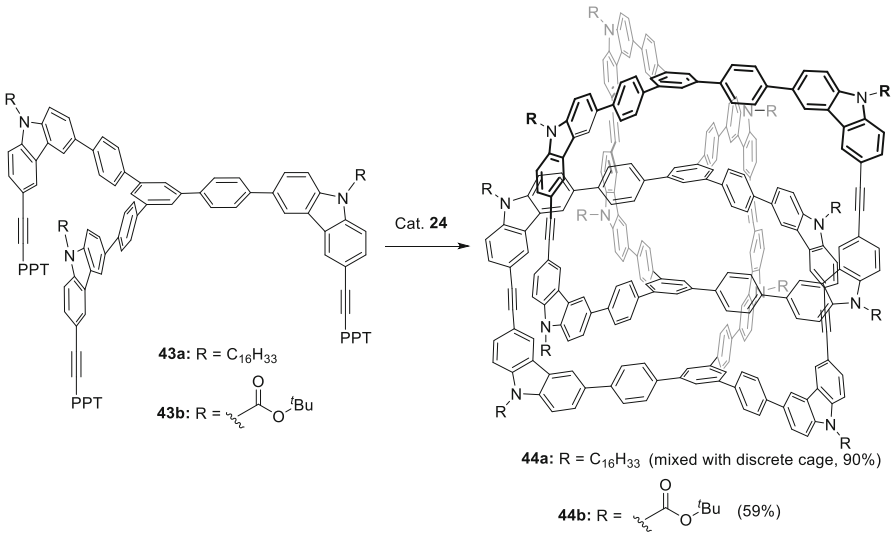

Scheme 8 Alkyne metathesis applied to monomer **43** to give an interlocked shape-persistent 3D macrocycle

of the alkyne metathesis method as a contemporary and evolving synthetic technique.

4 Conclusion

While alkyne metathesis holds clear advantages to conventional cross-coupling techniques, the majority of poly(aryleneethynylene) syntheses still rely on more traditional mechanistically irreversible methods such as Sonogashira coupling. It is clear, however, that these PAEs hold increasing significance as functional materials, and by integrating the alkyne metathesis technique with the polymer chemists' portfolio of synthetic tools, more superior and facile ethynylene-based materials could be realized.

We see the limiting factor in all this to be primarily the availability of robust and user-friendly catalytic systems that support alkyne metathesis. This should be evident from the shortage of new catalysts designed over the past 5 years, and so we would highlight this issue as one of the major hurdles to overcome in this field to date. Overall, however, poly(aryleneethynylene) systems have proved promising as functional materials from their expanding library of diverse monomers to their vast number of tailorable parameters which continue to advance PAE polymers in many growing materials applications.

Acknowledgements This work was supported by National Science Foundation (DMR-1055705) and University of Colorado Renewable and Sustainable Energy Institute (RASEI).

References

1. Liu J, Lam JWY, Tang BZ (2009) Chem Rev 109:5799. doi:10.1021/cr900149d
2. Bunz UHF (2000) Chem Rev 100:1605. doi:10.1021/Cr990257j
3. Bunz UHF, Seehafer K, Bender M, Porz M (2015) Chem Soc Rev 44:4322. doi:10.1039/C4CS00267A
4. Juan Z, Swager TM (2005) oly(Arylene Etynylene)S From Synth Appl 177:151. doi:10.1007/b101377
5. Zhang W, Moore JS (2007) Adv Synth Catal 349:93. doi:10.1002/adsc.200600476
6. Fürstner A (2013) Angew Chem Int Ed 52:2794. doi:10.1002/anie.201204513
7. Schrock RR (2002) Chem Rev 102:145
8. Mortreux A, Coutelier O (2006) J Mol Catal A: Chem 254:96. doi:10.1016/j.molcata.2006.03.054
9. Wu XA, Tamm M (2011) Beilstein J Org Chem 7:82. doi:10.3762/Bjoc.7.12
10. Cotts PM, Swager TM, Zhou Q (1996) Macromolecules 29:7323. doi:10.1021/ma9602583
11. Bunz UHF (2001) Acc Chem Res 34:998. doi:10.1021/ar010092c
12. Weder C, Sarwa C, Bastiaansen C, Smith P (1997) Adv Mater 9:1035. doi:10.1002/adma.19970091308
13. Kim J, McHugh SK, Swager TM (1999) Macromolecules 32:1500. doi:10.1021/ma981774r
14. Rodríguez R, Quiñoá E, Riguera R, Freire F (2016) J Am Chem Soc 138:9620. doi:10.1021/jacs.6b04834
15. Bunz UHF (2000) Chem Rev 100:1605. doi:10.1021/cr990257j
16. Bunz UHF, Imhof JM, Bly RK, Bangcuyo CG, Rozanski L, Vanden Bout DA (2005) Macromolecules 38:5892. doi:10.1021/ma050854+
17. Miteva T, Palmer L, Kloppenburg L, Neher D, Bunz UHF (2000) Macromolecules 33:652. doi:10.1021/ma9912397

18. Seehafer K, Bender M, Bunz UHF (2014) Macromolecules 47:922. doi:10.1021/ma402615q
19. Sluch MI, Godt A, Bunz UHF, Berg MA (2001) J Am Chem Soc 123:6447. doi:10.1021/ja0159012
20. Kim J, Swager TM (2001) Nature 411: 1030. doi:10.1038/35082528
21. Kokil A (2015) Poly(Arylene Ethynylene)s. In: Kobayashi S, Müllen K (eds) Encyclopedia of polymeric nanomaterials. Springer, Berlin
22. Weder C (2005) Advances in polymer science, vol 177. Springer, Berlin
23. Montali A, Smith P, Weder C (1998) Synth Met 97:123. doi:10.1016/S0379-6779(98)00120-9
24. Joo S-H, Jeong M-Y, Ko DH, Park J-H, Kim KY, Bae SJ, Chung IJ, Jin J-I (2006) J Appl Polym Sci 100:299. doi:10.1002/app.23107
25. Palai AK, Kumar A, Mishra SP, Patri M (2014) J Mater Sci 49:7408. doi:10.1007/s10853-014-8438-2
26. Huang W, Chen H (2013) Macromolecules 46:2032. doi:10.1021/ma302576p
27. Brizius G, Pschirer NG, Steffen W, Stitzer K, zur Loye H-C, Bunz UHF (2000) J Am Chem Soc 122:12435. doi:10.1021/ja0010251
28. Schenning APHJ, Tsipis AC, Meskers SCJ, Beljonne D, Meijer EW, Brédas JL (2002) Chem Mater 14:1362. doi:10.1021/cm0109185
29. Wilson JN, Windscheif PM, Evans U, Myrick ML, Bunz UHF (2002) Macromolecules 35:8681. doi:10.1021/ma025616i
30. Chu Q, Pang Y, Ding L, Karasz FE (2003) Macromolecules 36:3848. doi:10.1021/ma034028h
31. Tong M, Sheng CX, Yang C, Vardeny ZV, Pang Y (2004) Phys Rev B 69:155211
32. Lu S-L, Yang M-J, Bai F-L (2004) Macromol Rapid Commun 25:968. doi:10.1002/marc.200400004
33. Daniel A, Egbe hN, Serdar Sariciftci N (2011) J Mater Chem 21:1338
34. Egbe DAM, Carbonnier B, Birckner E, Grummt U-W (2009) Prog Polym Sci 34:1023. doi:10.1016/j.progpolymsci.2009.03.003
35. Feier HM, Reid OG, Pace NA, Park J, Bergkamp JJ, Sellinger A, Gust D, Rumbles G (2016) Adv Energy Mater 6:1502176. doi:10.1002/aenm.201502176
36. Pascoe AR, Yang M, Kopidakis N, Zhu K, Reese MO, Rumbles G, Fekete M, Duffy NW, Cheng Y-B (2016) Nano Energy 22:439. doi:10.1016/j.nanoen.2016.02.031
37. Park J, Reid OG, Rumbles G (2015) J Phys Chem B 119:7729
38. Kastner C, Susarova DK, Jadhav R, Ulbricht C, Egbe DAM, Rathgeber S, Troshin PA, Hoppe H (2012) J Mater Chem 22:15987. doi:10.1039/C2JM32629A
39. Yang X, Kajiyama S, Fang J, Xu F, Uemura Y, Koumura N, Hara K, Orita A, Otera J (2012) Bull Chem Soc Jpn 85:687
40. Yang X, Fang J, Suzuma Y, Xu F, Orita A, Otera J, Kajiyama S, Koumura N, Hara K (2011) Chem Lett 40:620
41. Mammen M, Choi S-K, Whitesides GM (1998) Angew Chem Int Ed 37:2754. doi:10.1002/(SICI)1521-3773(19981102)37:20<2754:AID-ANIE2754>3.0.CO;2-3
42. Zhou Q, Swager TM (1995) J Am Chem Soc 117:12593. doi:10.1021/ja00155a023
43. Yang J-S, Swager TM (1998) J Am Chem Soc 120:11864. doi:10.1021/ja982293q
44. Rose A, Zhu Z, Madigan CF, Swager TM, Bulovic V (2005) Nature 434: 876. doi:10.1038/nature03438
45. Swager TM (2008) Acc Chem Res 41:1181. doi:10.1021/ar800107v
46. He G, Yan N, Yang J, Wang H, Ding L, Yin S, Fang Y (2011) Macromolecules 44:4759. doi:10.1021/ma200953s
47. Altınok E, Smith ZC, Thomas SW (2015) Macromolecules 48:6825. doi:10.1021/acs.macromol.5b01076
48. Bunz UHF, Seehafer K, Geyer FL, Bender M, Braun I, Smarsly E, Freudenberg J (2014) Macromol Rapid Commun 35:1466. doi:10.1002/marc.201400220
49. Zou X, Ren H, Zhu G (2013) Chem Commun 49:3925. doi:10.1039/C3CC00039G
50. Xu Y, Jin S, Xu H, Nagai A, Jiang D (2013) Chem Soc Rev 42:8012. doi:10.1039/C3CS60160A
51. Holst JR, Trewin A, Cooper AI (2010) Nat Chem 2:915
52. Jiang J-X, Su F, Trewin A, Wood CD, Campbell NL, Niu H, Dickinson C, Ganin AY, Rosseinsky MJ, Khimyak YZ, Cooper AI (2007) Angew Chem Int Ed 46:8574. doi:10.1002/anie.200701595
53. Dawson R, Laybourn A, Clowes R, Khimyak YZ, Adams DJ, Cooper AI (2009) Macromolecules 42:8809. doi:10.1021/ma901801s
54. Dawson R, Laybourn A, Khimyak YZ, Adams DJ, Cooper AI (2010) Macromolecules 43:8524. doi:10.1021/ma101541h

55. Lu W, Wei Z, Yuan D, Tian J, Fordham S, Zhou H-C (2014) Chem Mater 26:4589. doi:10.1021/cm501922h
56. Zhang Y, Zhang Y, Sun YL, Du X, Shi JY, Wang WD, Wang W (2012) Chem A Eur J 18:6328. doi:10.1002/chem.201103028
57. Lu G, Yang H, Zhu Y, Huggins T, Ren ZJ, Liu Z, Zhang W (2015) J Mater Chem A 3:4954. doi:10.1039/C4TA06231K
58. Sonogashira K, Tohda Y, Hagihara N (1975) Tetrahedron Lett 16:4467. doi:10.1016/S0040-4039(00)91094-3
59. Yang H, Jin Y, Du Y, Zhang W (2014) J Mater Chem A 2:5986. doi:10.1039/C3TA14227B
60. Zhu Y, Yang H, Jin Y, Zhang W (2013) Chem Mater 25:3718. doi:10.1021/cm402090k
61. Yang H, Zhu Y, Du Y, Tan D, Jin Y, Zhang W (2017) Mater Chem. Frontiers. doi:10.1039/c6qm00359a
62. Deraedt C, d'Halluin M, Astruc D (2013) Eur J Inorg Chem 2013:4881. doi:10.1002/ejic.201300682
63. Furstner A, Davies PW (2005) Chem Commun. doi:10.1039/B419143A
64. Pennella F, Banks RL, Bailey GC (1968) Chem Commun (London). doi:10.1039/C19680001548
65. Mortreux A, Blanchard M (1974) J Chem Soc Chem Commun. doi:10.1039/C39740000786
66. Moulijn JA, Reitsma HJ, Boelhouwer C (1972) J Catal 25:434. doi:10.1016/0021-9517(72)90245-X
67. Mortreux A, Petit F, Blanchard M (1978) Tetrahedron Lett 19:4967. doi:10.1016/S0040-4039(01)85783-X
68. Du Plessis JAK, Vosloo HCM (1991) J Mol Catal 65:21. doi:10.1016/0304-5102(91)85081-C
69. Vosloo HCM, du Plessis JAK (1998) J Mol Catal A Chem 133:205. doi:10.1016/S1381-1169(98)00089-2
70. Devarajan S, Walton DRM, Leigh GJ (1979) J Organomet Chem 181:99. doi:10.1016/S0022-328X(00)85740-X
71. Villemin D, Cadiot P (1982) Tetrahedron Lett 23:5139. doi:10.1016/S0040-4039(00)85779-2
72. Nishida M, Shiga H, Mori M (1998) J Org Chem 63:8606. doi:10.1021/jo981240o
73. Neil Gregory Pschirer UHFB (1999) Tetrahedron Lett 40:2481
74. Bly RK, Dyke KM, Bunz UHF (2005) J Organomet Chem 690:825. doi:10.1016/j.jorganchem.2004.10.038
75. Mortreux A, Petit F, Blanchard M (1980) J Mol Catal 8:97. doi:10.1016/0304-5102(80)87009-X
76. Maraval V, Lepetit C, Caminade A-M, Majoral J-P, Chauvin R (2006) Tetrahedron Lett 47:2155
77. Sashuk V, Ignatowska J, Grela K (2004) J Org Chem 69:7748
78. Schrock RR (1986) Acc Chem Res 19:342. doi:10.1021/ar00131a003
79. Jose Sancho RSS (1982) J Mol Catal 15:75
80. Schrock RR, Clark DN, Sancho J, Wegrovius JH, Rocklage SM, Pedersen SF (1982) Organometallics 1:1645
81. Katz TJ, McGinnis J (1975) J Am Chem Soc 97:1592. doi:10.1021/ja00839a063
82. Tsai Y-C, Diaconescu PL, Cummins CC (2000) Organometallics 19:5260. doi:10.1021/om000644f
83. Blackwell JM, Figueroa JS, Stephens FH, Cummins CC (2003) Organometallics 22:3351. doi:10.1021/om0301482
84. Fürstner A, Mathes C, Lehmann CW (1999) J Am Chem Soc 121:9453. doi:10.1021/ja991340r
85. Peters CJ, Odom AL, Cummins CC (1997) Chem Commun. doi:10.1039/A704251E
86. Zhang W, Kraft S, Moore JS (2003) Chem Commun. doi:10.1039/B212405J
87. Zhang W, Kraft S, Moore JS (2004) J Am Chem Soc 126:329. doi:10.1021/ja0379868
88. Zhang W, Lu Y, Moore JS (2007) Organic syntheses. Wiley, Hoboken
89. Yang H, Liu Z, Zhang W (2013) Adv Synth Catal 355:885. doi:10.1002/adsc.201201105
90. Jyothish K, Zhang W (2011) Angew Chem Int Ed Engl 50:3435. doi:10.1002/anie.201102678
91. Du Y, Yang H, Zhu C, Ortiz M, Okochi KD, Shoemaker R, Jin Y, Zhang W (2016) Chem Eur J 22:7959. doi:10.1002/chem.201505174
92. Jyothish K, Wang Q, Zhang W (2012) Adv Synth Catal 354:2073. doi:10.1002/adsc.201200243
93. Jyothish K, Zhang W (2011) Angew Chem Int Ed 50:3435. doi:10.1002/anie.201007559
94. Hu K, Yang H, Zhang W, Qin Y (2013) Chem Sci 4:3649. doi:10.1039/C3SC51264A
95. McGowan KP, O'Reilly ME, Ghiviriga I, Abboud KA, Veige AS (2013) Chem Sci 4:1145. doi:10.1039/C2SC21750C
96. Roland CD, Li H, Abboud KA, Wagener KB, Veige AS (2016) Nat Chem 8: 791. doi:10.1038/nchem.2516 http://www.nature.com/nchem/journal/v8/n8/abs/nchem.2516.html - supplementary-information

97. Krouse SA, Schrock RR, Cohen RE (1987) Macromolecules 20:903. doi:10.1021/ma00170a033
98. Krouse SA, Schrock RR (1989) Macromolecules 22:2569. doi:10.1021/ma00196a004
99. Carnes M, Buccella D, Siegrist T, Steigerwald ML, Nuckolls C (2008) J Am Chem Soc 130:14078. doi:10.1021/ja806351m
100. Sedbrook DF, Paley DW, Steigerwald ML, Nuckolls C, Fischer FR (2012) Macromolecules 45:5040. doi:10.1021/ma300876q
101. Paley DW, Sedbrook DF, Decatur J, Fischer FR, Steigerwald ML, Nuckolls C (2013) Angew Chem Int Ed 52:4591. doi:10.1002/anie.201300758
102. Fischer FR, Nuckolls C (2010) Angew Chem Int Ed 49:7257. doi:10.1002/anie.201003549
103. Bellone DE, Bours J, Menke EH, Fischer FR (2015) J Am Chem Soc 137:850. doi:10.1021/ja510919v
104. von Kugelgen S, Bellone DE, Cloke RR, Perkins WS, Fischer FR (2016) J Am Chem Soc 138:6234. doi:10.1021/jacs.6b02422
105. Gross DE, Moore JS (2011) Macromolecules 44:3685. doi:10.1021/ma2006552
106. Gross DE, Discekici E, Moore JS (2012) Chem Commun 48:4426. doi:10.1039/C2CC30701D
107. Marsella MJ, Maynard HD, Grubbs RH (1997) Angew Chem Int Ed Engl 36:1101. doi:10.1002/anie.199711011
108. Jin Y, Wang Q, Taynton P, Zhang W (2014) Acc Chem Res 47:1575. doi:10.1021/ar500037v
109. Zhang C, Wang Q, Long H, Zhang W (2011) J Am Chem Soc 133:20995. doi:10.1021/ja210418t
110. Zhang C, Long H, Zhang W (2012) Chem Commun 48:6172. doi:10.1039/C2CC32571C
111. Wang Q, Zhang C, Noll BC, Long H, Jin Y, Zhang W (2014) Angew Chem Int Ed 53:10663. doi:10.1002/anie.201404880
112. Yu C, Long H, Jin Y, Zhang W (2016) Org Lett 18:2946. doi:10.1021/acs.orglett.6b01293
113. Ortiz M, Cho S, Niklas J, Kim S, Poluektov OG, Zhang W, Rumbles G, Park J (2017) J Am Chem Soc. doi:10.1021/jacs.7b00220
114. Lee S, Yang A, Moneypenny TP, Moore JS (2016) J Am Chem Soc 138:2182. doi:10.1021/jacs.6b00468
115. Wang Q, Yu C, Zhang CX, Long H, Azarnoush S, Jin YH, Zhang W (2016) Chem Sci 7:3370. doi:10.1039/c5sc04977f
116. Wang Q, Yu C, Long H, Du Y, Jin Y, Zhang W (2015) Angew Chem Int Ed 54:7550. doi:10.1002/anie.201501679